Supporting information

Hydrogenated Oxygen Deficient Blue Anatase as Anode for High Performance Lithium Batteries

Jing Zheng, [a] *Yousong Liu,* [a] *Guangbin Ji,* [a]* *Peng Zhang,* [b] *Xingzhong Cao,* [b] *Baoyi Wang,* [b] *Chuhong Zhang,* [c]* *Xuguang Zhou,* [d] *Yan Zhu,* [d] *and Daning Shi* [d]

[a]College of Materials Science and Technology, Nanjing University of Aeronautics and Astronautics, Nanjing 210016, P. R. China

[b]Key Laboratory of Nuclear Analysis Techniques, Institute of High Energy Physics, Chinese Academy of Sciences, Beijing 100049, P. R. China

[c]State Key Lab of Polymer Materials Engineering, Polymer Research Institute, Sichuan University, Chengdu, 610065, P. R. China

[d]College of Science, Nanjing University of Aeronautics and Astronautics, Nanjing 211100, P. R. China

* Corresponding authors:

E-mail: gbji@nuaa.edu.cn (G.B. Ji) and chuhong.zhang@scu.edu.cn (C.C. Zhang)

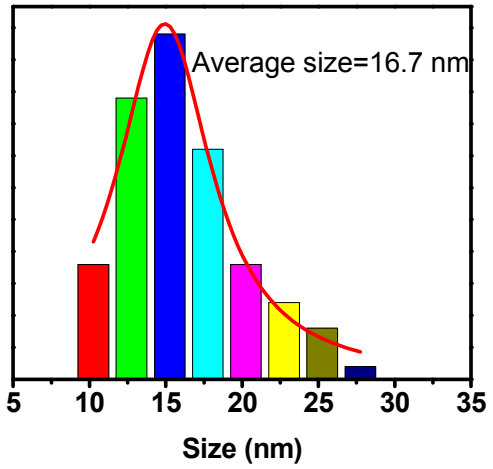

Figure S1. The particle size distribution of H-TiO_2-500.

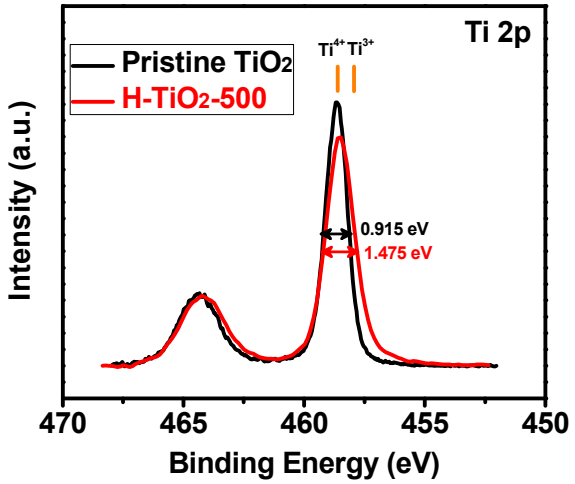

Figure S2. The original XPS curves of Ti 2p for the pristine TiO_2 and H-TiO_2-500.

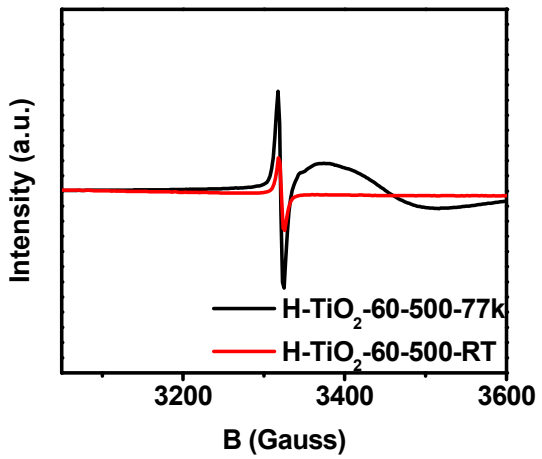

Figure S3. Low-temperature and room-temperature electron paramagnetic resonance (EPR) spectra of H-TiO_2-500.

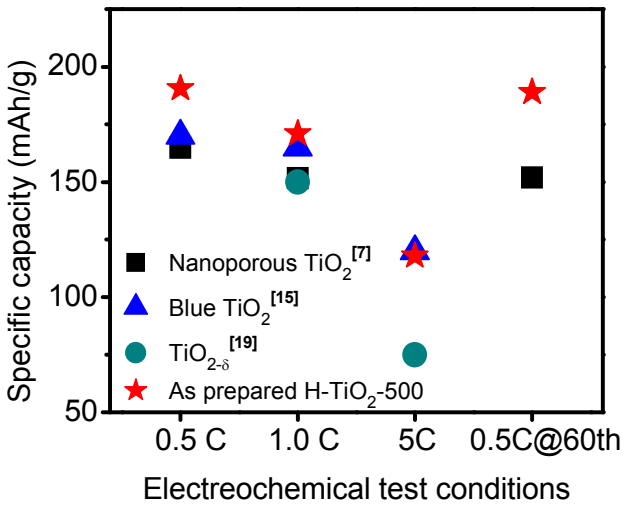

Figure S4. Comparison of the electrochemical property of the as-prepared H-TiO_2-500 (★) with reported nanoporous TiO_2[7] (■), blue TiO_2[15] (▲) and $TiO_{2-\delta}$[19] (●).

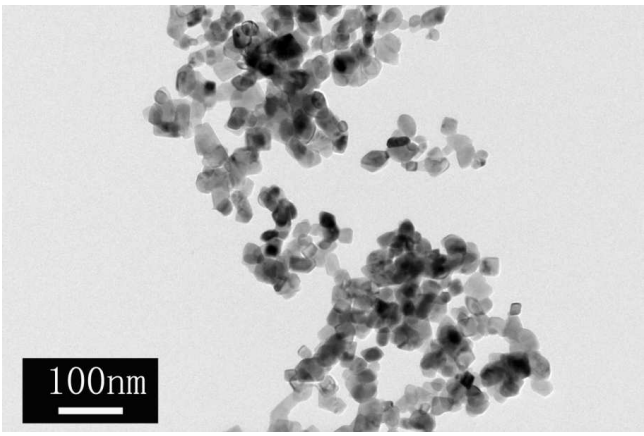

Figure S5. TEM image of the as-prepared TiO_2-17nm-R sample.

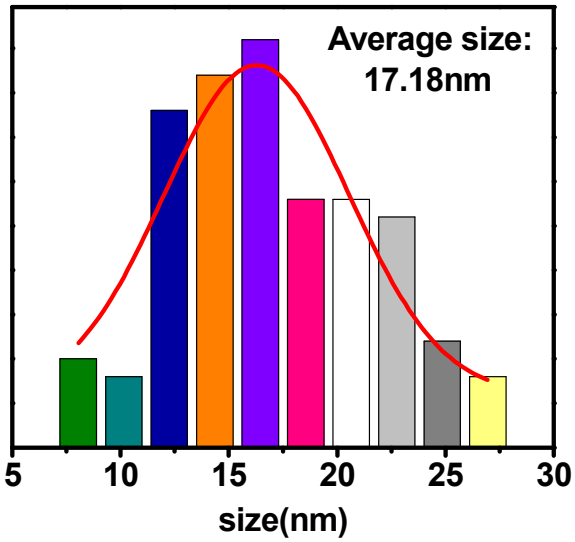

Figure S6. The particle size distribution of the as-prepared TiO_2-17nm-R sample.

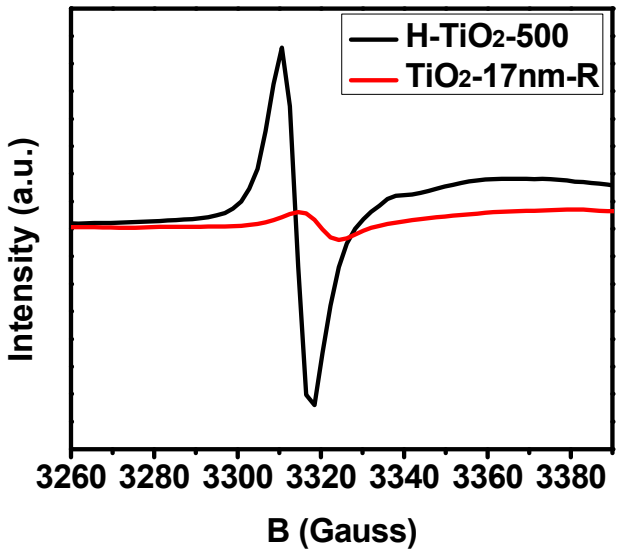

Figure S7. The low-temperature (77K) EPR spectra of the as-prepared TiO_2-17nm-R sample and H-TiO_2-500 sample. As it is indicated, the blue H-TiO_2-500 sample gives rise to a very strong EPR signal of g_1= 2.0010 and g_2= 1.9478, which can be attributed to the oxygen vacancy and Ti^{3+}, respectively. On the contrary, only weak signals were seen from the TiO_2-17nm-R. The TEM and EPR results directly proved that we have already synthesized the sample of 17 nm TiO_2 nanoparticle without oxygen vacancy/Ti^{3+}.

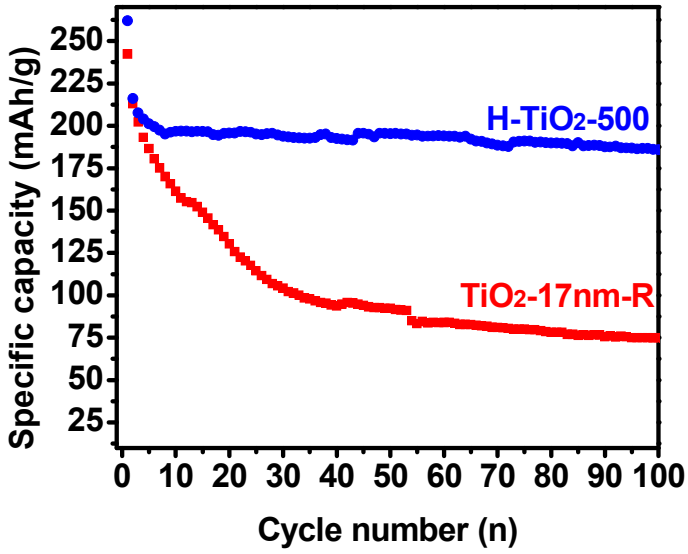

Figure S8. The cycling performance up to 100 cycles at 0.5C of the as-prepared TiO_2-17nm-R and H-TiO_2-500 sample. Even though these two samples have the same particle size of about 17nm, H-TiO_2-500 demonstrates much more stable cycling performance and much higher reversible capacities of 186 mAh/g even after 100 cycles than that of TiO_2-17nm-R with only 55.5 mAh/g.

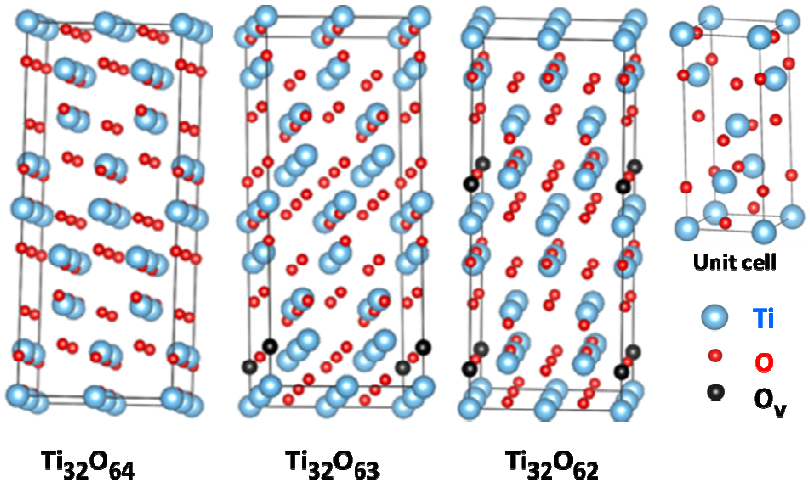

Figure S9. The corresponding stereogram of DFT calculation models for $Ti_{32}O_{64}$ (bulk TiO_2), $Ti_{32}O_{63}$ (1.56% oxygen deficiency) and $Ti_{32}O_{62}$ (3.13% oxygen deficiency), respectively.

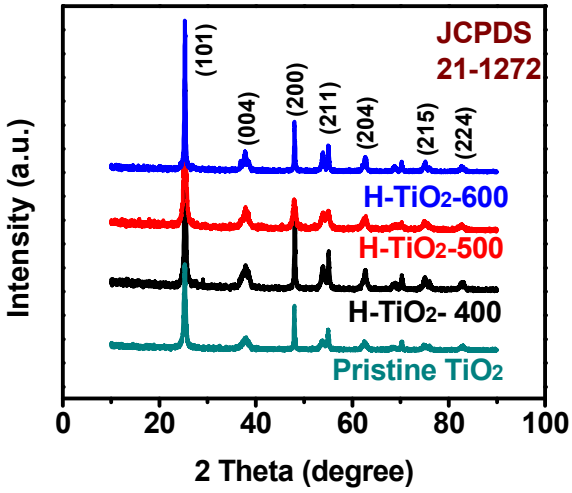

Figure S10. XRD of pristine TiO_2 and hydrogenated H-TiO_2 at different hydrogenation temperatures.

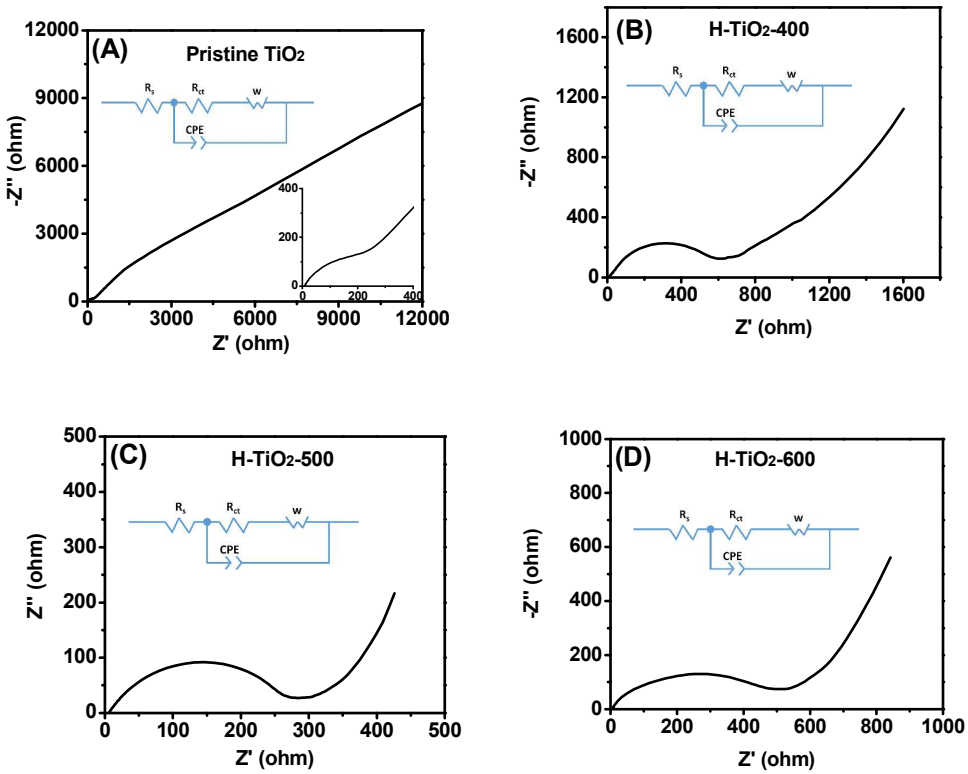

Figure S11. EIS spectra of pristine TiO_2 and hydrogenated H-TiO_2 at different hydrogenation temperatures. The inset for each is the proposed models of the equivalent circuits

Table S1. Fitted impedance parameters of pristine TiO_2 and hydrogenated H-TiO_2 at different hydrogenation temperatures via the model in Figure S7.

Samples	R_s (ohm)	R_{ct} (ohm)	W (ohm)
Pure TiO_2	8.24	299.3	0.6097
H-TiO_2-400	9.19	637.8	0.49954
H-TiO_2-500	6.08	264.5	0.38684
H-TiO_2-600	4.42	408.0	0.3283